

SELECTION OF AN INTERVAL FOR MASSIVE HYDRAULIC STIMULATION IN WELL DP 23-1, DESERT PEAK EAST EGS PROJECT, NEVADA

Ann Robertson-Tait¹, Susan Juch Lutz², Judith Sheridan³ and Christy L. Morris⁴

¹GeothermEx, Inc., Richmond, California, USA (e-mail: art@geothermex.com)

²Energy and Geoscience Institute, Salt Lake City, Utah, USA (e-mail: sjlutz@egi.utah.edu)

³GeoMechanics International, Palo Alto, California, USA (e-mail: judith@geomi.com)

⁴ORMAT Nevada Inc., Sparks, Nevada, USA (e-mail: cmorris@ormat.com)

ABSTRACT

As part of a DOE-industry cost-shared EGS project at Desert Peak East, Nevada, the feasibility of performing a massive hydraulic stimulation on an existing dry hole (DP 23-1) is being investigated. Using cuttings from this well and cores from a nearby hole, the stratigraphic sequence in the project area has been re-evaluated. Furthermore, detailed information on lithology and mineralogy in well DP 23-1 has been derived from a systematic examination of cuttings, using petrography and X-ray diffraction techniques. A wellbore image log obtained over a significant portion of the open hole has been analyzed in terms of the distribution and orientation of natural fractures and borehole failure phenomena (tensile fractures and breakouts). The features analyzed from the image log are compared with lithology, mineralogy, drilling rate and other geophysical logs to help determine the most prospective interval for stimulation.

INTRODUCTION

ORMAT Nevada Inc. (ORMAT) has received funding from the US Department of Energy (DOE) on a cost-shared basis to investigate the technical and economic feasibility of creating an artificial geothermal reservoir in the eastern part of the Desert Peak geothermal field. This project has as its ultimate goal the development of 2 - 5 MW of EGS-derived power from a stand-alone binary power plant supplied by 2 - 4 wells. Focusing initially on well DP 23-1, a hot but tight hole about 1.5 miles east of the producing hydrothermal wells at Desert Peak (Figure 1), a systematic evaluation of the EGS potential of this area is underway. This Phase I evaluation includes:

- 1) evaluation of existing geological data, including new petrologic evaluation of DP 23-1 and a nearby corehole (35-13 TCH);
- 2) review of previously collected geophysical data;
- 3) mechanical testing of cores from 35-13 TCH;

4) determining stress field and fracture orientations using a new wellbore image log run in DP 23-1;

5) conducting an injection test of well DP 23-1 to determine baseline (pre-stimulation) well and reservoir characteristics;

6) conceptual modeling, with a focus on the EGS portion of the field;

7) numerical modeling to enable estimation of required fracture densities and approximate well locations/configurations to support commercial production; and

8) preparation of a detailed plan to guide the next activities at the field (Phase II).

Continuation funding was recently approved to re-complete well DP 23-1 prior to stimulation, develop a water supply for stimulation and operation, and determine the magnitude of the minimum horizontal stress in the interval of interest, which lies within the pre-Tertiary basement rock.

PRE-TERTIARY STRATIGRAPHY

A simplified lithologic column for DP 23-1 is presented in Figure 2. Formation picks were developed based on mud log data, the interpretation presented below, and geophysical logs collected at the time of drilling in 1979.

As noted in Lutz *et al.* (2003), the pre-Tertiary metamorphic section in DP 23-1 is formed of two distinct subgroups with a sharp contact between them. The upper subgroup (pT1), which covers a depth range of 3,260 to 5,060 feet, is dominated by marine metasediments that have undergone regional greenschist facies metamorphism. The lower subgroup (pT2) extends to 7,020 feet and is composed of a series of Jurassic/Triassic phyllite, schist and mafic-to-intermediate plutonic rocks, all more strongly metamorphosed than the pT1 section. This is underlain and intruded by a two-mica granodiorite that is similar to Cretaceous intrusive rocks typical of the Sierra Nevada batholith found to the west in Nevada and California.

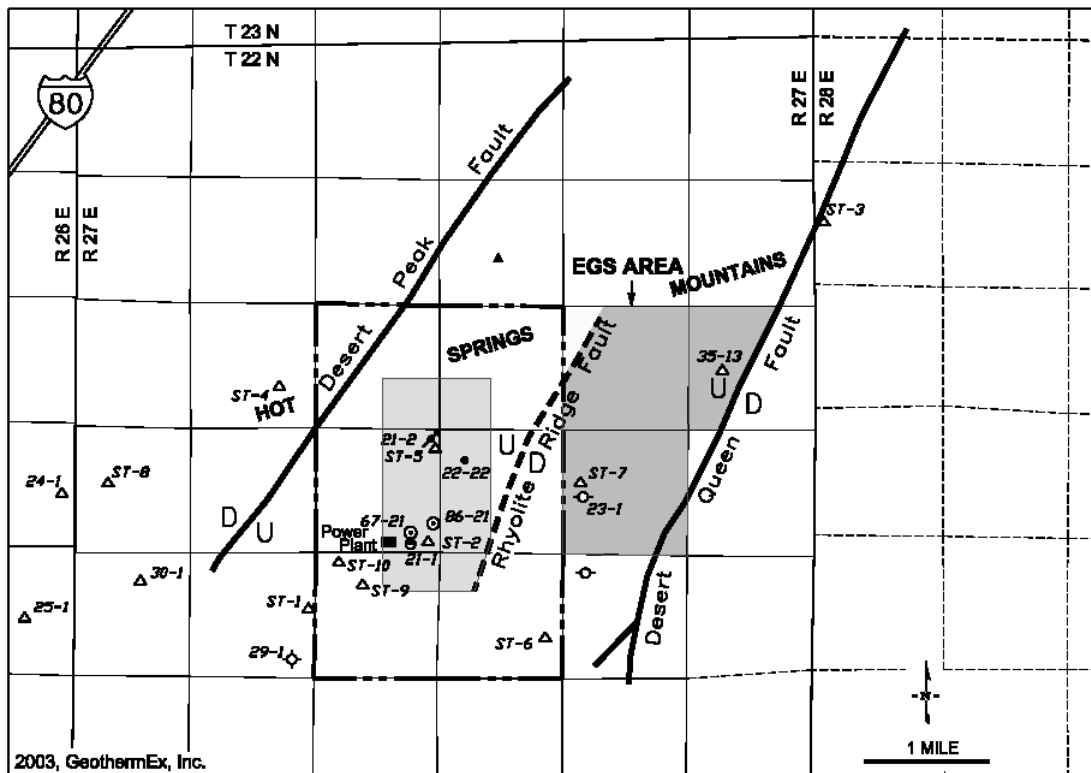


Figure 1: Desert Peak well location map

Several formations of interest from an EGS perspective were identified in the pT2 subgroup and below. The first is a quartz monzodiorite extending from 5,060 feet to 5,380 feet in well DP 23-1 (formation 5, Figure 2), which was also found in 35-13 TCH from 3,123 to 3,484 feet. The second is a hornblende diorite unit extending from 6,800 feet to 7,020 feet in well DP 23-1 (formation 7); this is not observed in 35-13 TCH owing to the relatively shallow depth of the core hole. Beneath these units is a third formation of interest: a two-mica granodiorite (referred to herein simply as granodiorite) that is less altered, less veined and more massive than the two intrusive units above. Thin dikes near the bottom of 35-13 TCH imply the presence of this granodiorite beneath the bottom the core hole (Lutz *et al.*, 2003).

Hydrothermal Alteration History

As discussed in Lutz *et al.* (2003), the basement rocks in the Desert Peak EGS area are composed of multiple intrusions of different ages and have undergone several episodes of metamorphism and

hydrothermal alteration. Magmatic-hydrothermal alteration minerals are related to intrusion of the granodiorite. The oldest fractures contain secondary biotite, tourmaline and potassium feldspar, and likely formed at temperatures above 600°F (315°C). These mineral phases are replaced by or crosscut by younger veins with low-temperature (<350°F or 175°C) mineral phases, such as chalcedonic quartz, dolomite, hematite, calcite and kaolin, that are in thermal equilibrium with the current temperature regime in the wells (Lutz *et al.*, 2003).

A moderate temperature (430-460°F; 220-240°C) propylitic-phyllitic assemblage consisting of chlorite, pyrite, calcite, epidote and sericite is present in the granodiorite and overlying rocks in DP 23-1 (Figure 3; from Lutz *et al.*, 2003). The propylitic alteration appears to be younger than the magmatic-hydrothermal alteration and may represent cooling of the granite after its initial emplacement. The upper 1,000 feet of the granodiorite body is moderately sericitized. Most of the primary biotite and some of the hydrothermal biotite has undergone retrograde

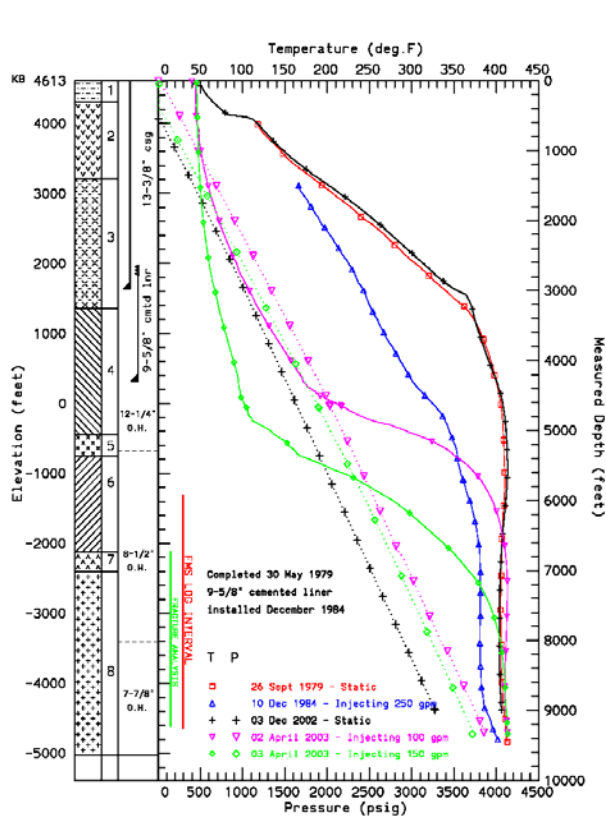


Figure 2: Lithology, completion and downhole survey data, well DP 23-1. April 2003 FMS log interval shown (lower left) by red line; data subset for fracture analysis shown by green line.

Formations: 1 – Truckee+Desert Peak;

2 - Chloropagus Formation; 3 - Rhyolite Unit; 4 - pT1 Metasediments; 5 - Quartz Monzodiorite (pT2); 6 - pT2 Metasediments; 7 - Hornblende Diorite (pT2); 8 - Two-Mica Granodiorite (see Lutz et al., 2003 for full descriptions of these units).

WELLBORE IMAGE LOG

Data Collection

Schlumberger’s “hot hole” Formation Microscanner (FMS) tool was run in well DP 23-1 after injecting for ~2.5 days to determine well and reservoir hydraulic parameters (see Sanyal et al., 2003) and to cool the well to ensure image quality. While running a TPS survey during the injection period, an obstruction was encountered at 5,850 feet in a section of pre-Tertiary phyllites and schists (formation 6A on Figure 2). This zone was sloughing into the hole during injection, and an increasing amount of fill was noted at bottomhole on subsequent tool runs. The FMS tool was run into the hole and began logging up from 9,265 feet (TD=9,641 feet); logging stopped at 5,924 feet to avoid encountering the obstruction with the tool arms open. Therefore, the upper quartz monzodiorite unit was not logged. However, wellbore images were obtained through most of the granodiorite and a portion of the overlying pT2 units (formation 6B on Figure 2).

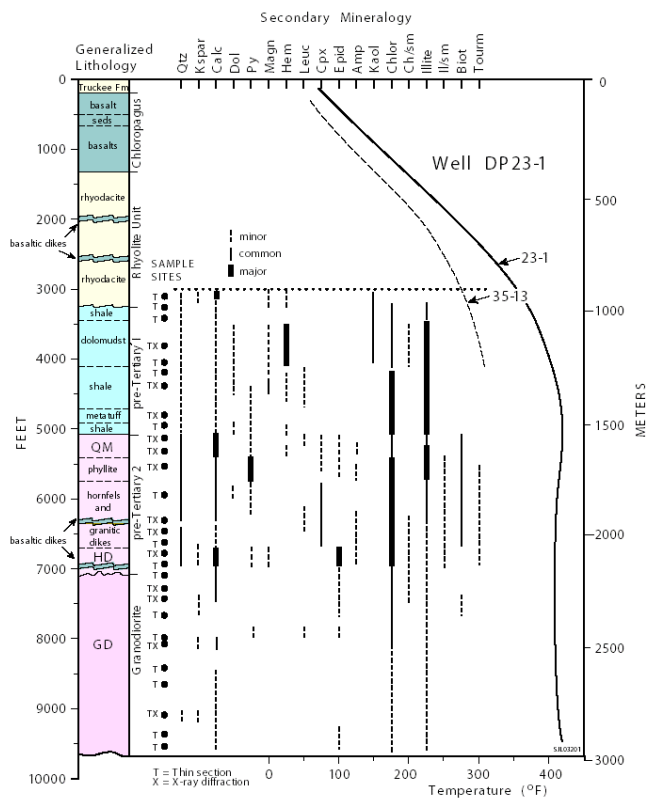


Figure 3: Primary lithology, secondary mineralogy and temperature in well DP 23-1 (from Lutz et al., 2003)

Data Analysis

The digital data for the FMS log were obtained from Schlumberger and provided to GeoMechanics International (GMI) for analysis, along with supporting data from the well, including previously collected geophysical logs, temperature logs, drilling data and well test data. Wellbore failure data were analyzed to determine stress field orientation and (in conjunction with other data) constrain the local stress tensor, and the fracture population was analyzed in a portion of the logged interval (6,730 to 9,228 feet).

Wellbore Failure Analysis

Figure 4 presents a summary of the observed wellbore failure data. Borehole breakouts were determined from both image data and caliper data (using the FMS tool arms); tensile cracks were identified from image data.

“Valid” breakouts determined from caliper data are defined as those that: 1) show a sufficiently large difference between the two caliper measurements; 2) occur when the logging tool is not spinning in the wellbore; 3) are not at the top or bottom of the wellbore; and 4) are not washouts or toolmarks, as identified by certain shape factors. A total of 52

valid breakouts were identified between 5,922 and 7,594 feet using the caliper data, and show a

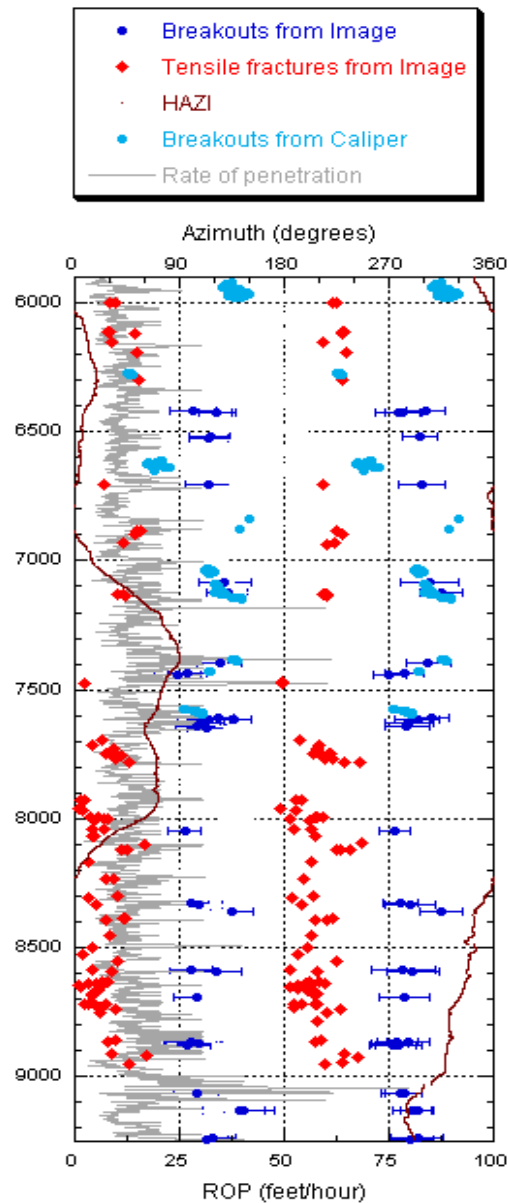


Figure 4: Observed wellbore failure features and drilling penetration rate (ROP), well DP 23-1

dominant direction of N128°E (39 breakouts) and a subordinate direction of N68°E (13 breakouts). As breakouts form at right angles to the direction of the maximum horizontal stress (S_{Hmax}), the dominant trend suggests an S_{Hmax} direction of N38°E. A total of 65 breakouts were identified between 6,418 and 9,241 feet using the image data; these suggest an S_{Hmax} direction of N27°E. A total of 170 tensile cracks were identified between 6,000 and 8,949 feet; these also suggest an S_{Hmax} direction of N27°E.

Analysis of Fractures

Owing to budget considerations, the fracture analysis used only a portion of the logged interval; as shown in Figure 2, this covered most of the granodiorite and extended about half way through the pT2 hornblende diorite unit above it. Nearly 11,000 fractures were identified in this interval; Figure 5 shows their orientation, while Figure 6 shows the magnitude and direction of dip. The dominant fracture direction is NNE, dips range from 30 – 75°, and the dominant dip directions are NW and SE.

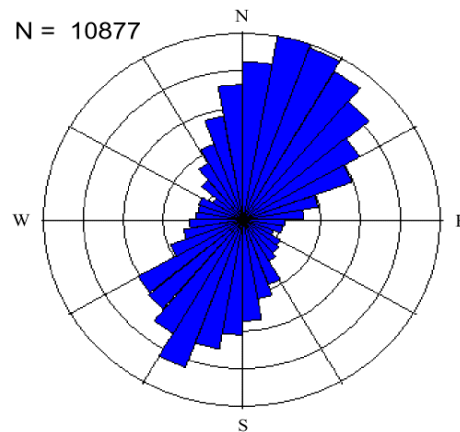


Figure 5: Orientation of natural fractures between 6,730 and 9,230 feet in well DP 23-1

DISCUSSION

The analysis of the recent log data leads to several observations:

- 1) The wellbore failure data and the dominant strike of natural fractures show a stress field orientation that is not only consistent between data sets but also reflects the current stress field as indicated by both regional and local geologic data (Faulds *et al.*, 2003).
- 2) Breakouts tend to occur where the drilling penetration rate is high (*i.e.*, in zones of weaker rock), while tensile cracks tend to occur where the drilling penetration rate is low (*i.e.*, in stronger rock).
- 3) Significantly more tensile cracks are observed below 7,600 feet than above it. Possible reasons for this include a greater amount of cooling in the portion of the well during drilling and injection, more quartz in the reservoir rock, and/or stronger rock overall below 7,600 feet.
- 4) Changes are noted in the dominant fracture dip direction with depth: from the top of the analyzed interval (at 6,730 feet) to ~7,350, NW dips are more

dominant; from 7,350 to 7,600 feet, SE dips are more common; no dominant direction is apparent between 7,600 and 7,750 feet (the number of identified fractures is also lower in this interval); NW dips predominate from 7,750 to 8,000 feet; SE and NW dips are more or less equal between 8,000 and 8,350 feet, below which the dominant dip direction is again SE.

5) The number of fractures per foot observed on the image log tends to decrease with depth, although this may be an artifact of image quality, since a lesser number of fractures are generally identified in intervals where the image quality is poorer (see Figure 6).

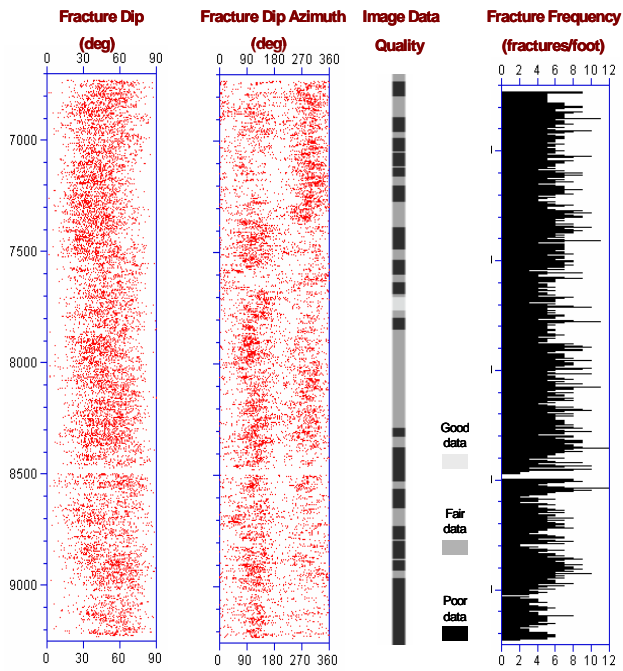


Figure 6: Analysis of natural fractures between 6,730 and 9,230 feet in well DP 23-1: dip magnitude, dip direction, FMS log data quality and fracture frequency.

The various data sets were compared to evaluate the possibility that changes in primary lithology and/or secondary mineralization may be correlated with some or all of these observations, or may otherwise be useful in selecting an interval for stimulation. As shown in Figure 3, there is an overall decrease in secondary mineralization passing from the pT2 units into the granodiorite. XRD analyses show that the granodiorite has a relatively consistent overall composition with depth, including quartz content. Illite is minor but constant through both the hornfelsic pT2 units and the upper part of the granodiorite. There is a consistent decrease in chlorite and illite with depth and an overall decrease in alteration and fracturing in the granodiorite below the lower shear zone at 7,650 feet. Caliper data show

the hole to be “out of gauge” to a greater degree, and to have a greater variation in hole diameter on the two tool arms above this shear zone, while below it, the caliper data show a more regular borehole. In addition, the upper, more sericitized granodiorite drills somewhat faster than the lower granodiorite. Taken together, the competence of the rock below the shear zone appears to be greater than that above it.

Our work so far has not revealed either a local or field-scale stratigraphic or structural explanation for the change in dominant dip direction with depth; recent mapping and gravity work (Faulds *et al.*, 2003) do not suggest that any of the block-rotating faults mapped at the surface intersect well DP 23-1 in the pT2 or the granodiorite. It is possible the deeper units are offset along older, buried structures, which might account for the observed variation in dip direction. However, these hypothesized structures do not appear in gravity data owing to low density contrast within the basement units.

TEMPERATURE AND SPINNER DATA

Although we set out to use geological and rock mechanical features to help define an interval for hydraulic stimulation, other data provide useful insights. A temperature survey conducted during injection after re-completing the well in 1984 (the blue survey in Figure 2) shows a permeable interval at approximately 9,000 feet, with an isothermal interval above it to a depth of 6,750 feet (near the top of the hornblende diorite). This survey was run after cleaning and circulating the hole, running and cementing the 9-5/8-inch liner (Figure 2), cleaning and circulating again (about 2 weeks were spent with the rig on the hole altogether), and injecting at about 5 barrels per minute for several hours.

Owing to the relatively low injection rate and short duration, the permeable zone at 9,000 feet cannot be identified in the two injecting temperature surveys from the pre-logging cooling period in April 2003 (Figure 2). However, the well went on vacuum after a day of injection, and was progressively cooling deeper and deeper. Spinner surveys run concurrently with the two injecting temperature surveys show different results (Figure 7): the later survey appears to indicate a fluid loss zone at or below 9,000 feet while the earlier does not. The reduction in spinner rate occurs within about 300 feet of the recently filled bottom of the well, leaving some ambiguity regarding its significance. Nevertheless, we believe this permeable zone exists, and that fluids will exit the well at deep levels during stimulation.

There is no sign that any preferential cooling took place around the shear zone at ~7,650 feet on any survey.

CONCLUSIONS

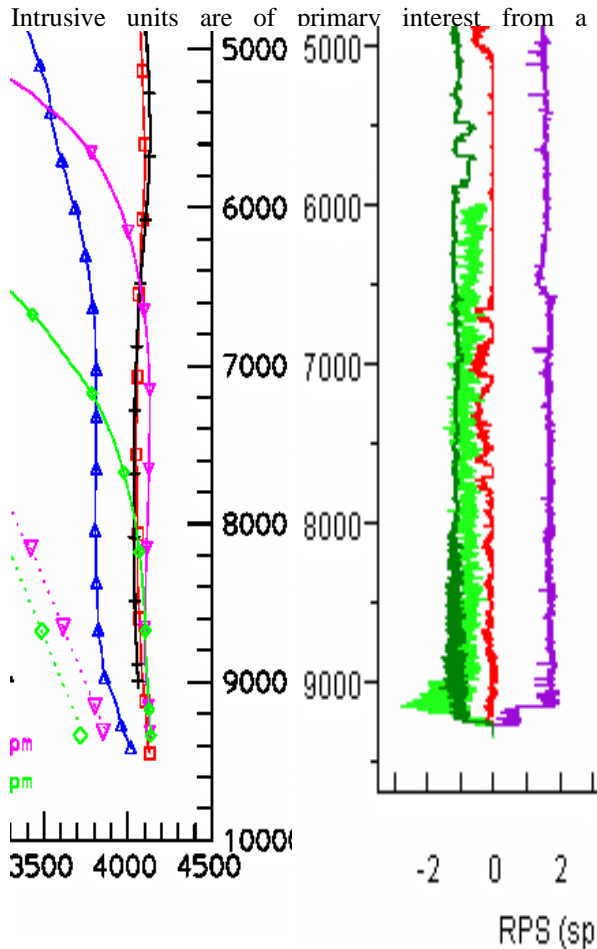


Figure 7: Temperature (left) and spinner (right) data from well DP 23-1 showing location of permeable zone at about 9,000 feet.

unstable during injection. The lowermost pT2 (a hornblende diorite, formation 7) and a deeper, younger granodiorite (formation 8) are more massive and look mechanically attractive. The granodiorite is less altered, particularly below a shear zone at 7,650 feet, where a significant increase in the number of tensile cracks is observed from the image log. The rate of penetration is slightly greater and the hole is more irregular above the shear zone than below. Taken together, this information suggests that the competence of the rock below the shear zone is

greater than that above it. For massive hydraulic stimulation, consideration is being given to the entire interval below the unstable phyllite or a more limited interval comprised of the lower portion of the granodiorite. In either case, stimulation should be facilitated by the presence of a zone of deep permeability at about 9,000 feet.

ACKNOWLEDGEMENTS

The authors gratefully acknowledge the support for this project from the U.S. Department of Energy, Assistant Secretary for Energy Efficiency and Renewable Energy, Geothermal Technologies program under a cooperative agreement with Golden Field Offices, DE-FC36-02ID14406 for EGS field projects.

REFERENCES

Faulds, J.E. and L.G. Garside, 2003. Preliminary geologic map of the Desert Peak-Brady geothermal fields, Churchill County, Nevada. Nevada Bureau of Mines and Geology Open-File Report 03-27.

Faulds, J.E., L.G. Garside and G. Oppliger, 2003. Structural analysis of the Desert Peak-Brady geothermal field, western Nevada: implications for understanding linkages between NE-trending structures and geothermal anomalies in the Humboldt Structural Zone. Transactions, Geothermal Resources Council, Vol. 27, pp. 859 – 864.

Lutz, S.J., A. Schriener Jr., D. Schochet and A. Robertson-Tait, 2003. Geologic characterization of pre-Tertiary rocks at the Desert Peak East EGS project site, Churchill County, Nevada. Transactions, Geothermal Resources Council, Vol. 27, pp.865-870.

Robertson-Tait, A., and C. Morris, 2003. Progress and future plans at the Desert Peak East EGS project. Transactions, Geothermal Resources Council, Vol. 27, pp. 871 - 877.

Sanyal, S.K., J.W. Lovekin, R.C. Henneberger, A. Robertson-Tait, P.J. Brown, C. Morris and D. Schochet, 2003. Injection testing for an Enhanced Geothermal Systems project at Desert Peak, Nevada. Transactions, Geothermal Resources Council, Vol. 27, pp. 885 – 891.